

ANTICANCER ACTIVITY AND CYTOTOXICITY OF ZnS NANOPARTICLES ON MCF-7 HUMAN BREAST CANCER CELLS

Marwa Salah¹, Mustafa Hammadi¹ and Esam H. Hummadi^{2*}

¹Department of Chemistry, College of Education for Pure Science, University of Diyala, Iraq.

²Department of Biotechnology, College of Science, University of Diyala, Iraq.

*e-mail : esam_hummadi@sciences.uodiyala.edu.iq

(Received 22 October 2020, Revised 30 January 2021, Accepted 8 February 2021)

ABSTRACT : Nanoparticles (NPs) are successfully used in medicine alternatively to anticancer agents. In this study, ZnS-NPs were synthesized by co-precipitation technique and characterized by using different methods including Infrared Spectra Measurements, X-Ray Diffraction (XRD), Energy-dispersive X-ray spectroscopy, Scanning electron microscope, and Atomic Force Microscopy. The FTIR showed broad absorption bands related to Zn-S. The XRD and SEM examination showed that the average size of ZnS particles sized 11.42 nm. SEM test showed sphere-shaped NPs with an average diameter of about 71 nm. The purity of the synthesized NPs measured by XRD was high. The cytotoxicity of ZnS was tested against MCF-7 cells at different concentrations. After 24 hr, the inhibition rate was 74.40% at 200 µg/ml and increased by half with increasing the concentration up to 400 µg/ml of 47.72%. The results showed an R square equal to 0.9906, which indicated a strong correlation between the variables. The half-maximal inhibitory concentration (IC₅₀) of zinc sulfide, measured after 24 hours was 379.9 µg/ml. Zinc sulfide nanoparticles have potential therapeutic properties as antitumor drugs based on the fact that they can slowly release heavy metal ions.

Key words : ZnS nanoparticles, MCF-7, co-precipitation method, cytotoxicity.

How to cite : Marwa Salah, Mustafa Hammadi and Esam H. Hummadi (2021) Anticancer activity and cytotoxicity of ZnS nanoparticles on MCF-7 human breast cancer cells. *Biochem. Cell. Arch.* **21**, 95-99. DocID: https://connectjournals.com/03896.2021.21.95

INTRODUCTION

Nanomaterial has made big changes in medical and clinical fields during the past decades (Khan *et al*, 2019; Wu *et al*, 2015). Each field of medicine has attracted growing interest from NPs due to their ability to deliver drugs in the optimal dosage range and contributing to increase drug therapeutic performance as well as their acceptable side effects (Bayal *et al*, 2019). This encourage the researchers to speculate in the cytotoxic impacts of organically sheltered nanomaterials against malignancy cells and the mechanical pathways of cell killing (Harada *et al*, 2013; Yang *et al*, 2012). In patients infected with breast tumors, the eliminated metastasis is an exceptionally risky stage which can causes about 90% mortality (Karuppaiya *et al*, 2010). Hence, the eradication of the cell metastasis is a promising technique to control the breast tumor spreading. Some nanomaterials are capable of selectively killing cancer cells, such as Ag, Au, ZnO, TiO₂ and MgO (Tran *et al*, 2016). Zinc sulphide

(ZnS) is one of the attractive substances possess a key applications in biology as protein sensors, cellular imaging, antibacterial agents and anticancer agents (Bayal *et al*, 2019). It has been studied because they have unusual chemical and physical properties such as high coefficient of electrochemical coupling, UV detection, catalysis, high photo-stability, and a wide range of radiation absorption (Tan *et al*, 2014; Bose *et al*, 2016). Also, ZnS are capable to reduce the cytotoxicity effects of quantum dotes in treatment of cancer diseases (Chibli *et al*, 2011; Tran *et al*, 2016; Bayal *et al*, 2019). Dash *et al* (2014) investigated the biological activity of ZnS-NPs on cancer cells. In a dose-dependent manner, they found that the cell viability and flow cytometric analysis demonstrated the potent cytotoxic effects of ZnS-NPs on the treated cells. Also, successful leukemic cell absorption of ZnS-NPs has been confirmed by phase contrast fluorescence microscopy (Dash *et al*, 2014). In a study carried out by Bose *et al* (2016), ZnS-NPs used at various concentrations in

primary mouse RPE (MRPE) cells. ZnS-NPs demonstrated dose-dependent cytotoxicity against MRPE cells with no changes were observed on the cells at low concentration. Also, the exposure of the MRPE cells to ZnS-NPs increased their permeability in dose- and time-dependent manner (Bose *et al*, 2016). In this study, ZnS nanoparticles were synthesized by co-precipitation technique and characterised to explore their bioactivity against MCF-7 human breast cancer cells in comparison with a commercial drug called Femara used anticancer to treat breast cancer disease.

MATERIALS AND METHODS

The chemicals used in this study were of analytical grade. Zinc (II) chloride hydrate $\text{ZnCl}_2 \cdot 2\text{H}_2\text{O}$, Sodium sulphide hydrate $\text{Na}_2\text{S} \cdot \text{H}_2\text{O}$, 96% ethanol was purchased from Alfa Assar (Germany). Polystyrene 96-well plates were purchased from Greiner Bio-One (Germany). Femara tablets (2.5 mg) were purchased from Novartis Pharmaceuticals (UK). MCF7 cell lines obtained from (ATCC® HTB-22™, USA).

Synthesis and characterization

Preparation of zinc sulphide nanoparticles

A 0.5 Molar of aqueous zinc chloride $\text{ZnCl}_2 \cdot 2\text{H}_2\text{O}$ was prepared by dissolving 3.8 g of the salt in 50 ml deionized water and mixed using a magnetic stirrer for 30 minutes until completely dissolve. Sodium sulphide solution $\text{Na}_2\text{S} \cdot \text{H}_2\text{O}$ 0.5 M was prepared by dissolving 2.4 g of the chemical in 50 ml deionized water. Aliquot of 20 ml of sodium sulphide solution was added by dropping into the zinc chloride solution with monitoring the pH at 6 for 1 hr until a dark nutty precipitate appear. The precipitate was separated by centrifugation at 2000 rpm/min for 5 min. The resulted sediment was washed with ethanol and deionized water few times. Lastly, the product

was dried at 80 °C for 4 hr. Fig. 1 shows a diagram of zinc sulphide NPs synthesis.

Characterization techniques

The zinc sulphide nanoparticles were characterized by numerous strategies included X-ray diffraction (XRD), Fourier-transform infrared (FTIR) spectroscopy and Scanning electron microscope (SEM). Crystallite size of the synthesized nanoparticles was determined by using XRD (Shimadzu, Kyoto, Japan). Miniflex X-ray diffractometry including Cu-K α radiations ($\lambda = 0.15406$ nm) of the 2θ extent beyond 20° after 80°C . FTIR spectra of the samples was conducted using Shimadzu (Tokyo, Japan). FTIR spectrophotometer using KBr pellet. SEM examination was carried out by 200 kV Zeiss SEM (Germany).

MTT assay for zinc sulphide nanoparticles

This assay was carried out using MTT dye (10 mg/ml) (3-[4,5-dimethylthiazole-2-yl]-2,5-diphenyltetrazolium bromide). Metal sulphide nanoparticles sample was dissolved in 0.2% DMSO to get a gradient concentrations of 25, 50, 100, 200, 400 $\mu\text{g}/\text{ml}$. Aliquot of 200 μl suspended cells (1×10^4 cell/well) prepared in RPMI medium was dispersed in 96-Microplate and incubated at 37°C for 24 hr in the presence of 5% CO_2 . The cell cultures were treated with 20 μl of ZnS-NPs and further incubated for 24 hr under the same conditions. Then, 10 μl of MTT reagent was added into each sample and incubated for 5 hr at 37°C . The absorbance was measured at 570 nm using DANA-3200 ELISA READER. Two controls were used in this test: control-1 consisted of DMSO+cells and control-2 consisted of untreated cells only. The inhibition percentage and IC_{50} were calculated and analysed statistically.

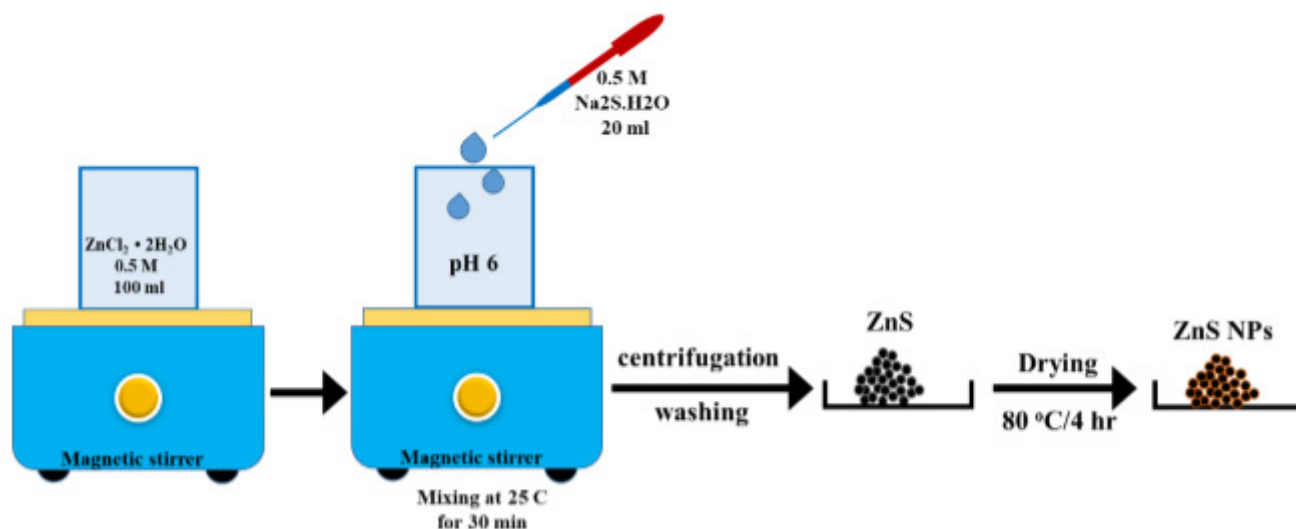


Fig. 1 : Preparation steps of zinc sulphide nanoparticles by co-precipitation method.

Statistical analysis

The results of zinc sulphide nanoparticles activity on MCF-7 cells were analyzed statistically using Graph Pad Prism 8.0. One way ANOVA was applied to conclude the means at a significance level of $P < 0.05$. All the experiments were conducted at least two times with three replicates for each under the same conditions.

RESULTS AND DISCUSSION

Morphological analysis

ZnS-NPs were prepared by the co-precipitation technique. The crystal structure and phase purity of the prepared nanoparticles were characterized by X-ray diffraction as shown in Fig. 2. The X-ray diffraction spectrum was matched the standard spectrum of zinc sulphide according to the JCPDS card 79-2204 ZnS database. The sulphide formation was detected Crystalline ZnS by diffraction peaks at (10.04, 22.3, 27.02, 31.64, 44.22, 51.56, 55.46, 61.94, 73.04). No impurities were observed in the X-ray diffraction spectrum of ZnS nanoparticles.

The average crystal size of the nanoparticles was calculated at 11.42 nm using the Debye-Scherrer formula as shown in equation below and Table 1 (Ramasamy *et al*, 2012).

$$D = \frac{K\lambda}{\Delta \cos\theta}$$

FTIR study

The infrared spectra of the aqueous zinc chloride salt ($\text{ZnCl}_2 \cdot 2\text{H}_2\text{O}$) used in the preparation of ZnS-NPs were recorded before the reaction as shown in Fig. 3A after formatting them as tablets with cesium iodide (CsI) and within the range of $400\text{-}4000\text{ cm}^{-1}$. The locations of absorption bands for a selection of active groups were determined and an attempt was made to interpret them based on what was stated in the literature, noting the changes occurring in these bands in shape and intensity, as salt spectra of aqueous zinc chloride showed absorption bands at $3450, 1600, 550.22\text{ cm}^{-1}$. The absorption band 3450 cm^{-1} returns to the stretching

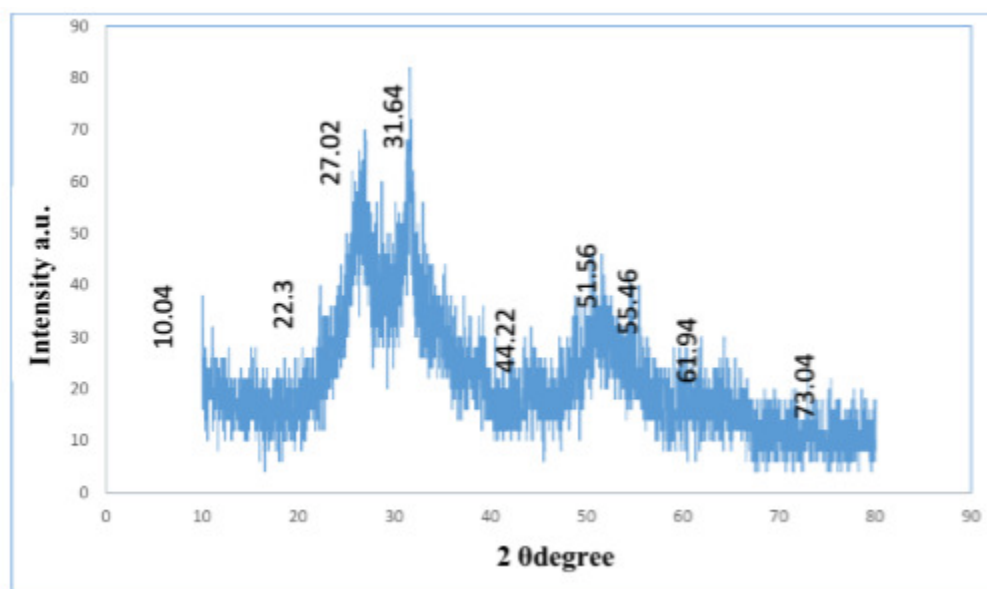


Fig. 2 : X-ray diffraction spectrum of ZnS nanoparticles.

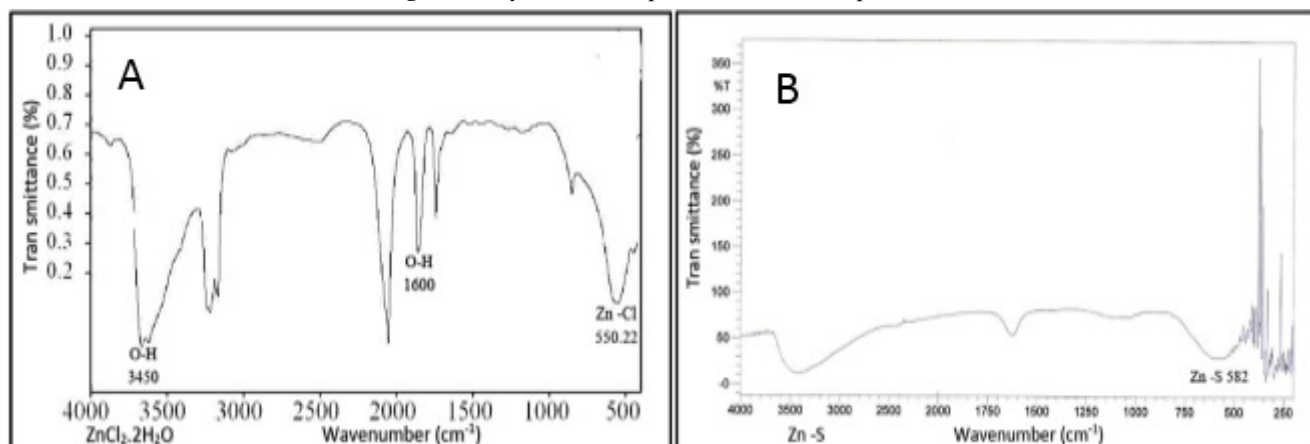


Fig. 3 : The infrared spectrum of aqueous zinc chloride (A) and ZnS nanoparticles (B).

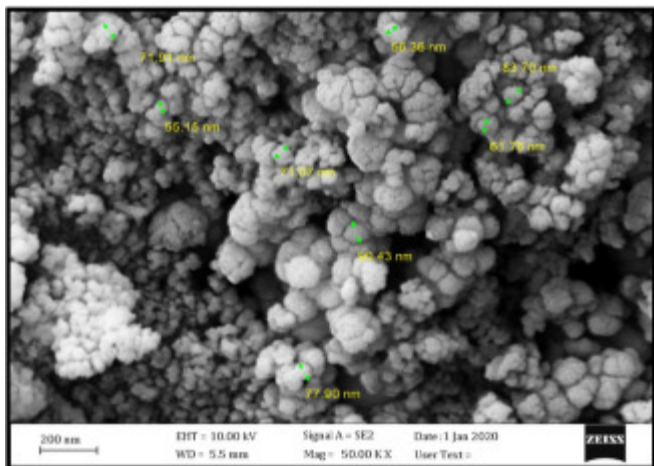


Fig. 4 : SEM image of synthesized ZnS nanoparticles.

nanoparticles were prepared in the nanometer range. The SEM images indicated that some of the nanoparticles were well separated from each other while most of them were present in an agglomerated form. This agglomeration is due to the electrostatic effects in addition to the effect of the aqueous suspension, which reveals the behavior of this nanoparticle clumping is consistent with the behavior similar to the clumping of nanoparticles in previous studies and the average diameter of these particles is about 71 nm (Devi *et al*, 2007).

Cytotoxicity of ZnS-NPs

The MTT test was conducted to determine the cytotoxicity of nanostructured zinc sulphide particles on

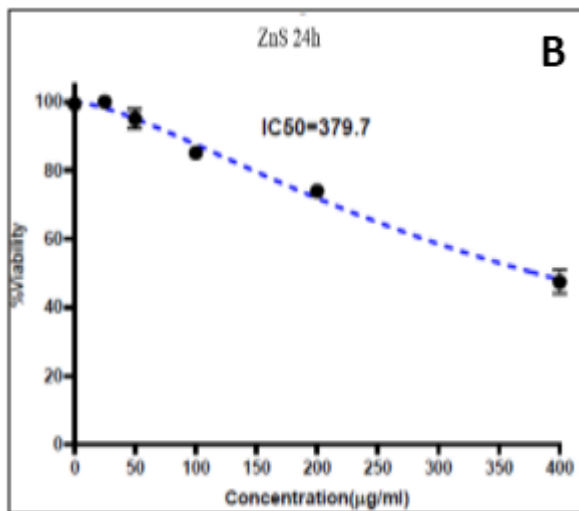
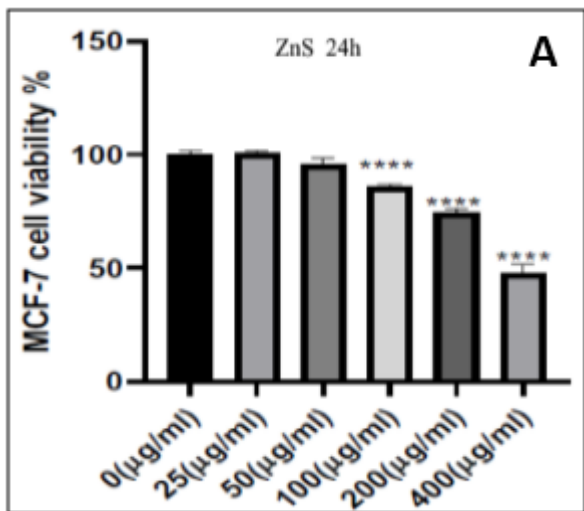


Fig. 5 : Cell viability at different concentrations of ZnS-NPs assessed by MTT dye after 24 hr incubation with the cell line (A) and IC₅₀ of ZnS-NPs (B).

Table 1 : The average size of crystalline account for the zinc sulphide nanoparticles by Debye-Scherer Law.

| K | $\tilde{\epsilon}$ (Å) | Peak No. | Peak position 2 $\tilde{\epsilon}$ (°) | FWHM B size (°) | Dp (nm) | Dp Average (nm) |
|-----|------------------------|----------|--|-----------------|---------|-----------------|
| 0.9 | 1.54059 | 23 | 31.6913 | 0.54 | 15.29 | 11.42 |
| | | 18 | 26.5883 | 0.84 | 9.72 | |
| | | 17 | 25.8495 | 0.88 | 9.26 | |

vibrations of the hydroxyl group (O⁻ H), while the absorption beam 1600cm⁻¹ returns to the bending vibrations of the hydroxyl group (O⁻ H) and the absorption beam 550.22 cm⁻¹ returns to the vibrations of the stretch Zn-Cl, while the infrared spectrum of the prepared zinc sulphide shows the presence of a new absorption beam at 582 cm⁻¹ is the extended vibration range of ZnS. These data are very consistent with the information from the published literature as shown in Fig. 3B (Farooqi *et al*, 2014).

SEM analysis

The morphological and structural properties of the ZnS nanoparticles were observed using a Scanning electron microscope (SEM). Fig. 4 shows that the

MCF-7 human breast cancer cell lines. The cytotoxicity was examined at different concentrations ranged from 25 to 400 µg/ml. The results showed that the viability of MCF-7 cells after 24 hr of treatment with 25 µg/ml ZnS-NPs was 99.98%, which indicates that the cancer cells did not affect anymore with NPs. However, the survival rate of MCF-7 cells at a concentration of 50 µg/ml was decreased to 95.66%, which indicates that there is a relationship between the dose increasing and the rate of cell inhibition. The highest decreasing rate in cell viability of MCF-7 was 47.72% at 400 µg/ml as shown in Fig. 5A. The half-maximal inhibitory concentration (IC₅₀) of nano-sized zinc sulphide was measured on MCF-7 breast cancer cells after 24 hr of incubation using a normalized

response. The IC₅₀ value was 379.9 µg/ml (R square 0.9835) as shown in Fig. 5B. Sulphide nanoparticles can significantly induce apoptosis in human Hep G2 and HL-60 cells with a very low value of IC₅₀ and little toxic effects on normal cells (Balaz *et al.*, 2012). Tran *et al.* (2016) demonstrated that ZnS nanoparticles can inhibit the metastasis of MCF-7-SCs in a dose-dependent manner by suppressing epithelial-mesenchymal transition process of the cells. However, they did not observe any toxicity effect of ZnS on the migration and invasion of MCF-7-SCs at a concentration of 400 µg/ml (Tran *et al.*, 2016).

CONCLUSION

In the current work, we described synthesise of ZnS via a cheap and practical co-precipitation method. The characterization of the structural properties of ZnS-NPs was carried out using FTIR, XRD, and SEM. Zinc sulphide nanoparticles have potential therapeutic activities as antitumor compounds because of its ability to slowly release heavy metal ions. The cell viability assay suggested that ZnS nanoparticles inhibited the metastasis of MCF-7 by suppressing the Epithelial-mesenchymal gait (EMT) process. This study revealed the potential utility of ZnS nanoparticles towards the inhibition of cell migration and invasion in breast cancer stem cells that can be used in breast cancer treatment.

REFERENCES

- Balaz P, Sedláč J, Pastorek M, Cholužová D, Vignarooban K, Bhosle S and Stalder B (2012) Arsenic sulphide As₄S₄ nanoparticles: Physico-chemical properties and anticancer effects. *J. Nano Research* **18**, 149-155.
- Bayal M, Janardhanan P, Tom E, Chandran N, Devadathan S, Ranjeet D and Nair S S (2019) Cytotoxicity of nanoparticles-Are the size and shape only matters? or the media parameters too?: a study on band engineered ZnS nanoparticles and calculations based on equivolume stress model. *Nanotoxicol.* **13**(8), 1005-1020.
- Bose K, Lakshminarasimhan H, Sundar K and Kathiresan T (2016) Cytotoxic effect of ZnS nanoparticles on primary mouse retinal pigment epithelial cells. *Artificial cells, Nanomedicine and Biotechnology* **44**(7), 1764-1773.
- Cao Y, Wang H J, Cao C, Sun Y Y, Yang L, Wang B Q and Zhou J G (2011) Inhibition effects of protein-conjugated amorphous zinc sulphide nanoparticles on tumor cells growth. *J. Nanoparticle Res.* **13**(7), 2759-2767.
- Chang Y N, Zhang M, Xia L, Zhang J and Xing G (2012) The toxic effects and mechanisms of CuO and ZnO nanoparticles. *Materials* **5**(12), 2850-2871.
- Chibli H, Carlini L, Park S, Dimitrijevic N M and Nadeau J L (2011) Cytotoxicity of InP/ZnS quantum dots related to reactive oxygen species generation. *Nanoscale* **3**(6), 2552-2559.
- Dash S K, Ghosh T, Roy S, Chattopadhyay S and Das D (2014) Zinc sulphide nanoparticles selectively induce cytotoxic and genotoxic effects on leukemic cells: involvement of reactive oxygen species and tumor necrosis factor alpha. *J. Appl. Toxicol.* **34**(11), 1130-1144.
- Devi B R, Raveendran R and Vaidyan A V (2007) Synthesis and characterization of Mn²⁺-doped ZnS nanoparticles. *Pramana* **68**(4), 679-687.
- Farooqi M M H and Srivastava R K (2014) Structural, optical and photoconductivity study of ZnS nanoparticles synthesized by a low temperature solid state reaction method. *Materials Science in Semiconductor Processing* **20**, 61-67.
- Harada A, Ono M, Yuba E and Kono K (2013) Titanium dioxide nanoparticle-entrapped poly ion complex micelles generate singlet oxygen in the cells by ultrasound irradiation for son dynamic therapy. *Biomaterials Sci.* **1**(1), 65-73.
- Karuppaiya P, Satheeshkumar E, Chao W T, Kao L Y, Chen E C F and Tsay H S (2013) Anti-metastatic activity of biologically synthesized gold nanoparticles on human fibrosarcoma cell line HT-1080. *Colloids and Surfaces B: Biointerfaces* **110**, 163-170.
- Khan I, Saeed K and Khan I (2019) Nanoparticles: Properties, applications and toxicities. *Arabian J. Chem.* **12**(7), 908-931.
- Lin L, Xiong L, Wen Y, Lei S, Deng X, Liu Z and Miao X (2015) Active targeting of nano-photosensitizer delivery systems for photodynamic therapy of cancer stem cells. *J. Biomedical Nanotech.* **11**(4), 531-554.
- Ramasamy V, Praba K and Murugadoss G (2012) Study of optical and thermal properties in nickel doped ZnS nanoparticles using surfactants. *Superlattices and Microstructures* **51**(5), 699-714.
- Tan L, Huang C, Peng R, Tang Y and Li W (2014) Development of hybrid organic-inorganic surface imprinted Mn-doped ZnS QDs and their application as a sensing material for target proteins. *Biosensors and Bioelectronics* **61**, 506-511.
- Tran T A, Krishnamoorthy K, Cho S K and Kim S J (2016) Inhibitory effect of zinc sulphide nanoparticles towards breast cancer stem cell migration and invasion. *J. Biomedical Nanotech.* **12**(2), 329-336.
- Wu Y, Wang Z, Liu G, Zeng X, Wang X, Gao Y and Mei L (2015) Novel simvastatin-loaded nanoparticles based on cholic acid-core star-shaped PLGA for breast cancer treatment. *J. Biomedical Nanotech.* **11**(7), 1247-1260.
- Yang K, Wan J, Zhang S, Tian B, Zhang Y and Liu Z (2012) The influence of surface chemistry and size of nanoscale graphene oxide on photothermal therapy of cancer using ultra-low laser power. *Biomaterials* **33**(7), 2206-2214.